IEEE Open Journal of
Antennas and Propagation

Received 22 August 2020; revised 23 September 2020; accepted 25 September 2020. Date of publication 8 October 2020; date of current version 29 October 2020.

Digital Object Identifier 10.1109/OJAP.2020.3029534

Millimeter-Wave Butler Matrix Beamforming Circuit Using Finline in Double-Layer Dielectric Substrate

NGUYEN THANH TUAN [1] (Graduate Student Member, IEEE), KUNIO SAKAKIBARA [1] (Senior Member, IEEE), KOJIRO IWASA [2], TAKESHI OKUNAGA [2], NOBUYOSHI KIKUMA [1] (Senior Member, IEEE), AND YOSHIKI SUGIMOTO [1] (Member, IEEE)

[1]Department of Electrical and Mechanical Engineering, Nagoya Institute of Technology, Nagoya 466-8555, Japan

[2]Department of Process, Nippon Pillar Packing Company Ltd., Osaka 669-1333, Japan

CORRESPONDING AUTHOR: N. T. TUAN (e-mail: t.nguyen.794@stn.nitech.ac.jp)

ABSTRACT This article presents a new kind of finline in double-layer dielectric substrate and its beamforming circuit of Butler matrix in the millimeter-wave band. The finline is constructed by inserting a slotline between two dielectric substrate layers. In this configuration, it is bounded within a closed structure composed of a double-layer dielectric substrate and two rows of via-hole arrangement, contributing to low dispersion and low radiation loss of the finline characteristics. The proposed finline design aims to provide a low-complexity and low-loss transmission line which is applied to the Butler matrix design. A 4×4 Butler matrix for 4 switchable beams is realized by using the finline in the double-layer dielectric substrate. In addition, a waveguide-to-finline transition is developed as a feeding circuit for the Butler matrix. Characteristics of the proposed transition and the Butler matrix were analyzed by electromagnetic analysis of the finite element method and demonstrated by experiments at 79 GHz. The proposed Butler matrix obtains a wideband characteristic and an acceptable insertion loss of 2.42 dB. The array factor which is calculated from the measured amplitude and phase outputs 4 switchable beams with the beam directions of $+14°$, $-46.5°$, $+46.5°$ and $-14°$, respectively. The proposed beamforming circuit using finline in double-layer dielectric substrate would be attractive for millimeter-wave applications due to its performance and low cost.

INDEX TERMS Millimeter wave, transmission line transition, finline, multi-layer substrate, multi-beam antenna, beam steering, Butler matrix.

I. INTRODUCTION

RECENTLY, with a huge demand of wireless connected devices, the frequency spectrum of millimeter-wave band has been considered as an alternative solution for short-range communications with high-speed data transfer rates. Millimeter-wave technologies have been applied in various applications such as fixed wireless access [1], 5G mobile communication systems [2], and high angular resolution automotive radars [3]–[6]. Multibeam antennas can be applied to these systems to cover a wide range of transmission. Therefore, beamforming techniques become core solutions providing the beam steering capability in the multibeam antenna systems. Popular analog beamforming techniques include Blass matrix [7]–[8], Rotman lens [9], dielectric lens [10] and Butler matrix [11]. Among them, Butler matrix is widely used in beamforming circuits because of its low-loss nature and scalability in the number of beams.

Butler matrix is an $N \times N$ network which is composed of hybrid couplers, crossovers and phase shifters. The conventional Butler matrix is usually designed by microstrip line but it has disadvantage of high transmission loss. Several kinds of transmission lines have been proposed for the efforts of providing high transmission performance of the Butler matrix. For example, hollow waveguide Butler matrix [12], Butler matrices using single PCB [13], substrate integrated waveguide [14], complementary metal-oxide-semiconductor

(CMOS) [15] and multilayer stripline [16] technologies have been reported for transmission loss reduction. The hollow waveguide showed advantages of high transmission performance but the structure is complicated, costly and difficult to apply to Butler matrices in mass production.

Finline structure consists of a partially metalized dielectric substrate shielded by a metal waveguide enclosure and their characteristics have been discussed in [17]–[19]. The finline does not have a cut-off frequency, but has wideband and low loss characteristics and it is widely applied to millimeter-wave PIN diode switches. However, the metal waveguide structure is bulky in size and weight and it is not economical in manufacturing. Therefore, an alternative technique using multi-layer dielectric substrate waveguide is proposed to replace the metal waveguide in millimeter-wave applications.

Multi-layer dielectric substrate is a compact structure which can be constructed from printed circuits by build-up or low temperature co-fired ceramic (LTCC) technologies [20]. The idea of a simple finline structure in double-layer dielectric substrate has been proposed in previous works [21]–[25]. However, this work focuses on more detailed investigations of the finline characteristics on its parameters and waveguide-to-finline transition design. The proposed finline is bounded within a closed structure composed of upper and lower metal plates, and two rows of via-hole arrangement. The finline is realized by inserting a slotline between two dielectric substrate layers with the dominant propagation of longitudinal-section electric (LSE) and longitudinal-section magnetic (LSM) mode. A wave propagates along the finline, while the electric field is concentrated at the gap of the slotline. Consequently, the finline in double-layer dielectric substrate is capable of preventing radiation loss and the leakage power between via holes. The finline in double-layer dielectric substrate is not affected by the cut-off frequency, it can be applied in a wide frequency range and easy for integration with a compact size.

A design of 4×4 Butler matrix for 4 switchable beams realized by finline in double-layer dielectric substrate is provided in this article. Moreover, the Butler matrix characteristics are demonstrated by the fabricated prototype. In addition to that, the array factors of the Butler matrix are calculated to evaluate radiation pattern of the multi-beam antenna.

This article is organized as follows. The structure of the proposed finline in double-layer dielectric substrate and its charateristics are first discussed in Section II, followed by the analysis of the waveguide-to-finline transition in Section III. The detailed design procedure of the Butler matrix conducted by electromagnetic analysis of HFSS at 79 GHz [26] and its performance are discussed in Section IV. Finally, conclusion is then presented in Section V.

II. FINLINE IN DOUBLE-LAYER DIELECTRIC SUBSTRATE

Structure of the proposed finline in double-layer dielectric substrate is illustrated in Fig. 1(a). The finline consists of two separate dielectric substrate layers of fluorocarbon resin films ($\varepsilon_r = 2.16$, loss tangent $\tan\delta = 0.0005$), three printed

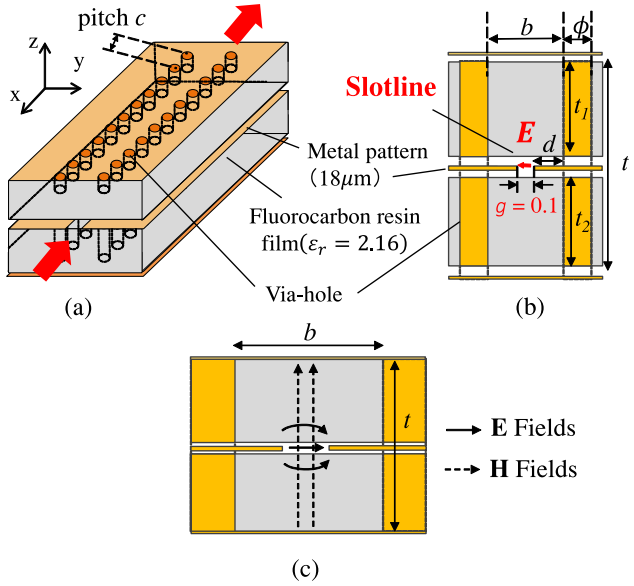

FIGURE 1. Structure of finline in double-layer dielectric substrate. (a) Overview, (b) yz plane, (c) LSM_{01} mode.

metal patterns (thickness: 18μm) and two rows of via-hole in parallel and through the dielectric substrates. A slotline (width $g = 0.1$ mm) is etched in the middle metal layer before it is shielded by two separate dielectric substrates. To create a closed structure of finline, two rows of via-hole are arranged through the dielectric substrates at a distance d from the edges of the slotline as the broad wall of the finline. The diameter of via hole $\phi = 0.30$ mm; pitch of via holes $c = 2\phi$ and $d = 0.35$ mm are required for possible fabrication. The proposed finline is formed as a shielded structure with the narrow wall b and the broad wall t as illustrated in Fig. 1(b). The narrow wall is determined as $b = 0.8$ mm. The broad wall t is the sum of two substrate thicknesses (t_1 and t_2) that are commercial product of NPC-H220A provided by NIPPON PILLAR PACKING CO., LTD [27]. t_1 and t_2 should not be greater than b to prevent the generation of waveguide mode in the closed space of each dielectric substrate. An investigation of finline characteristics depending on dielectric substrate thicknesses is conducted as shown in Fig. 2. When shielding structure ($t \times b$) is large, higher-order waveguide mode generates. With $t_1 = t_2 = 1.0$ mm, the higher-order mode tends to be generated in each dielectric substrate, followed by a reduction of transmission performance of the finline. When the thicknesses of 0.8mm and 0.6 mm are used, only a slight difference is observed in reflection and transmission characteristics. Selecting from the product list, the values of $t_1 = t_2 = 0.8$ mm are selected to build the broad wall of the finline ($t = 1.6$ mm).

The finline supports wave propagation of LSM_{01} mode. Plane wave in horizontal polarization concentrates at the slotline and propagates along the finline as illustrated in Fig. 1(c). The leakage wave in the horizontal polarization between via holes is cut off by copper foils at both sides of the finline, in which low dispersion can be achieved.

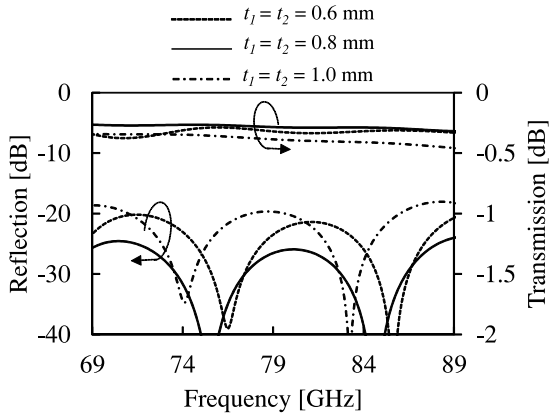

FIGURE 2. Finline characteristics depending on dielectric substrate thicknesses.

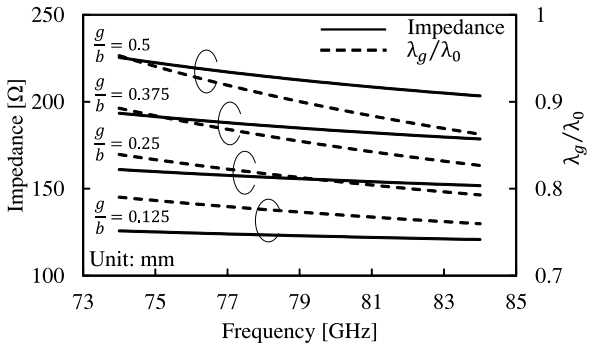

FIGURE 3. Characteristic impedance and wavelength ratio $\lambda g/\lambda_0$ versus frequency of finline.

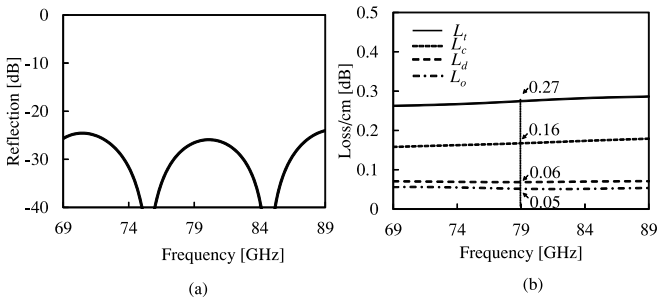

FIGURE 4. Reflection and transmission characteristics of proposed finline. (a) Reflection, (b) Transmission loss estimation.

The characteristic impedance and wavelength of the finline are necessary in the circuit design. They are controlled and determined by changing the slotline width g of the finline. By applying numerical analysis of finite element method, the characteristic impedance and wavelength ratio λ_g/λ_0 versus frequency of finline are calculated as shown in Fig. 3 (λ_g: wavelength of the finline in double-layer dielectric substrate). The characteristics show that the impedance is proportional to the width g of the slotline and the wavelength λ_g of the finline increases when the width g is extended. The slotline width g should be considered small to avoid the higher-order waveguide mode in the finline. In this design, $g = 0.1$ mm is selected for possible fabrication. The finline

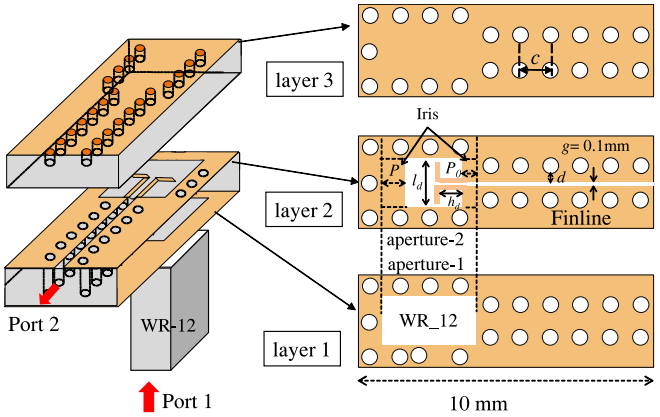

FIGURE 5. Structure of the proposed waveguide-to-finline transition.

TABLE 1. Parameters of the proposed waveguide-to-finline transition.

Parameters	Values (mm)	Values (λ)
Slotline width g	0.10	0.035
Dipole length l_d	1.26	0.5
Dipole height h_d	0.60	0.23
Iris length P	0.80	0.31
Iris length P_0	0.50	0.2
Thickness of dielectric substrate t_1	0.80	0.31
Thickness of dielectric substrate t_2	0.80	0.31
Distance from via hole edge to finline edge d	0.35	0.14
Diameter of via hole ϕ	0.30	0.12
Pitch of via holes c	0.60	0.23

has characteristic impedance of $Z_0 = 123\ \Omega$ and wavelength $\lambda_g = 2.9$ mm at 79 GHz.

The proposed finline is composed of a closed waveguide structure in double-layer dielectric substrate. Therefore, some advantages of low radiation loss and low electromagnetic interference can be expected in the finline characteristics. Simulated reflection and transmission characteristics of the proposed finline are presented in Fig. 4. The discrete arrangement of via holes in dielectric substrates causes reflected waves with the amplitude below -25 dB as shown in Fig. 4(a). The proposed finline structure is composed of dielectric substrates, metal plates and via holes. Therefore, the transmission loss (L_t) includes conductor loss (L_c), dielectric loss (L_d) and leakage loss (L_o). The loss factors of the proposed finline are calculated by HFSS as shown in Fig. 4(b). The total transmission loss of the proposed finline shows $L_t = 0.27$ dB/cm in which the loss factors are estimated as $L_c = 0.16$ dB/cm; $L_d = 0.06$ dB/cm and $L_o = 0.05$ dB/cm.

III. WAVEGUIDE-TO-FINLINE TRANSITION

A waveguide-to-finline transition is designed for integration between the finline and the hollow waveguide in millimeter-wave band. Metal layers of the proposed waveguide-to-finline transition are shown in Fig. 5. One end of the dielectric substrate is plugged with via holes to form a

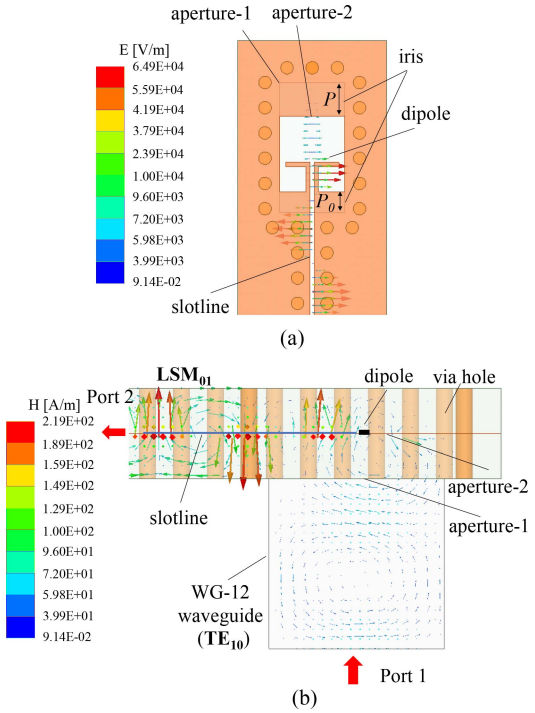

FIGURE 6. Field distributions of waveguide-to-finline transition at 79 GHz. (a) Electric field, (b) Magnetic field.

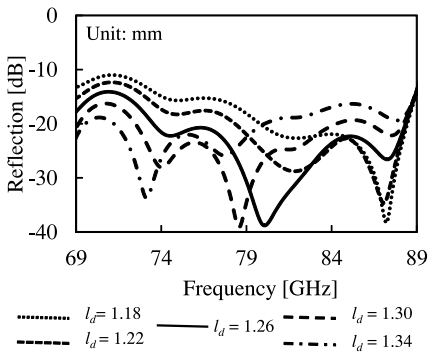

FIGURE 7. Reflection characteristics of waveguide-to-finline transition depending on l_d.

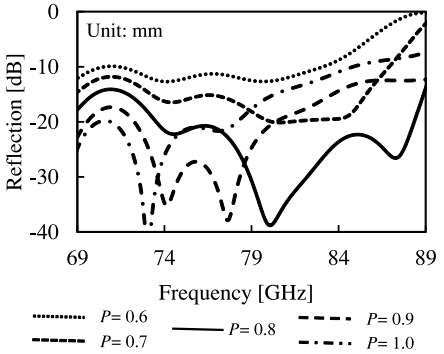

FIGURE 8. Reflection characteristics of waveguide-to-finline transition depending on iris length *P*.

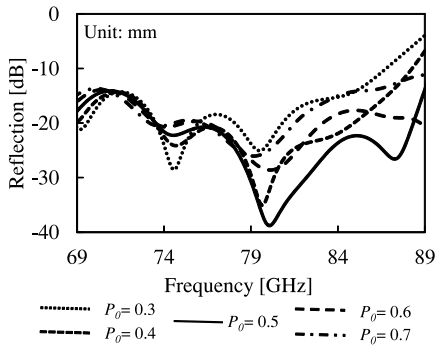

FIGURE 9. Reflection characteristics of waveguide-to-finline transition depending on iris length P_0.

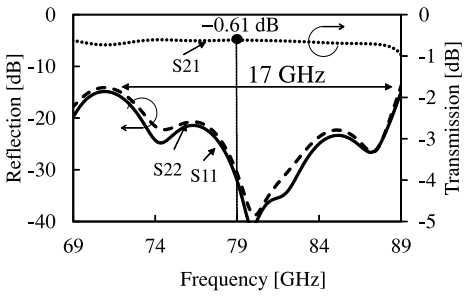

FIGURE 10. Simulated reflection and transmission characteristics of waveguide-to-finline transition.

short circuit for waveguide connection. A hollow rectangular waveguide is attached to layer 1 through an aperture-1 of WR-12 standard. A half-wavelength dipole antenna l_d which has an identical electrical polarization with the finline is proposed to be located at the aperture-2 and it is attached to the finline. For impedance matching between the hollow waveguide and dipole antenna, an iris is formed by extending the metal pattern by a distance P and P_0 from both ends of the waveguide at the aperture-2. In the transition, the electric field of TE_{10} mode from the hollow waveguide excites the dipole antenna as demonstrated in Fig. 6(a). Consequently, the dipole antenna positively excites the slotline of the finline due to the identical electrical polarization. The magnetic field of LSM_{01} mode is generated in the finline as illustrated in Figure 6(b). Finally, an electromagnetic wave is transmitted into the finline.

Center frequency of the proposed transition is controlled by the dipole length l_d as shown in Fig. 7. The center frequency is shifted toward the lower frequencies when the dipole length l_d is increased. In this transition design, the dipole length $l_d = 1.26$ mm is used to achieve center frequency at 79 GHz. By extending the iris length P, the coupling region of magnetic field changes, followed by the shift of center frequencies to lower frequencies as presented in Fig. 8. The iris length is optimized to be $P = 0.80$ mm so as to set the center frequency to 79 GHz. Iris length P_0 plays a role as a impedance matching section between the finline and the dipole. By adjusting iris length P_0, a slight shift of center frequency can be seen but reflection level changes significantly as presented in Fig. 9. The iris length is chosen as $P_0 = 0.50$ mm for the reflection level below -35 dB at 79 GHz.

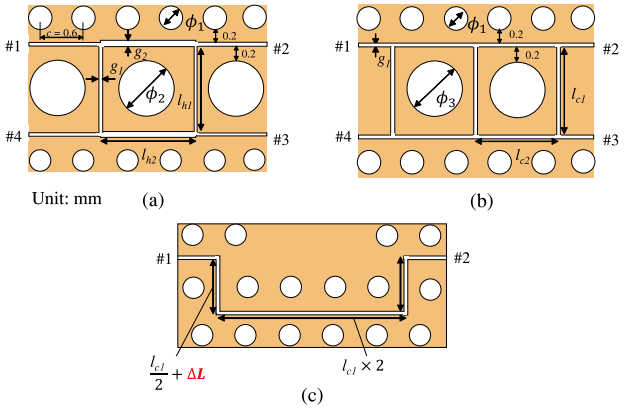

FIGURE 11. Structure of the Butler matrix components (on the middle metal layer of the double-layer substrate). (a) Hybrid coupler, (b) Crossover, (c) Phase shifter.

The optimum parameters of the proposed waveguide-to-finline transition are summarized in Table 1. In this transition, λ is the wavelength in dielectric. With these parameters, the reflection and transmission characteristics of the waveguide-to-finline transition are obtained as shown in Fig. 10. The proposed transition operates over a wide bandwidth of 17 GHz (21.5 %) at reflection level below -15 dB. The transmission loss at 79 GHz is 0.61 dB including 0.27 dB transmission loss of the finline. Therefore, the insertion loss of the proposed transition can be estimated as 0.34 dB.

IV. BEAMFORMING CIRCUIT OF BUTLER MATRIX

A. DESIGN PROCEDURE

The design procedure of the Butler matrix is given in this section. The Butler matrix structure consists of components such as hybrid couplers, crossovers and phase shifters. In this model, components of the Butler matrix are designed using the proposed finline configuration as shown in Fig. 11.

A hybrid coupler divides an RF signal from input port 1 to output ports 2 and 3 equally with 90° phase difference. It is laid out at the middle metal pattern of the double-layer substrate using two branch-lines with electrical length of l_{h1} and l_{h2} as shown in Fig. 11(a). In the finline hybrid coupler, characteristic impedances of branch-lines are investigated and determined by changing the widths g_1 and g_2 of the slotlines as in the discussion provided in Section II. In this design, g_1 and g_2 are 0.1 mm and 0.13 mm, respectively; electrical length of branch-lines are optimized in simulation as $l_{h1} = 0.96$ mm and $l_{h2} = 0.96$ mm for equal power division at output ports. Furthermore, due to some limitations in the fabrication process, space in the square of hybrid coupler is not enough to arrange some via holes $\phi_1 = 0.3$ mm with pitch of holes $c = 0.6$ mm, thus, one via hole with $\phi_2 = 0.55$ mm is placed in the square of hybrid coupler to ensure a unique distance of 0.2 mm between via holes and slotlines. Figure 12(a) indicates the simulated scattering parameters of the finline hybrid coupler. Reflection level of port 1 and isolation level of port 4 are below -20 dB at 79 GHz. The power is divided equally to port 2 and port 3

TABLE 2. Parameters of the Butler matrix components.

Parameters	Values (mm)
Slotline width g_1	0.10
Slotline width g_2	0.13
Branch-line length of hybrid circuit l_{h1}	0.96
Branch-line length of hybrid circuit l_{h2}	0.96
Branch-line length of crossover l_{c1}	0.88
Branch-line length of crossover l_{c2}	0.88
Line offset ΔL	-0.12, -0.05
Diameter of via hole ϕ_1	0.30
Diameter of via hole ϕ_2	0.55
Diameter of via hole ϕ_3	0.50

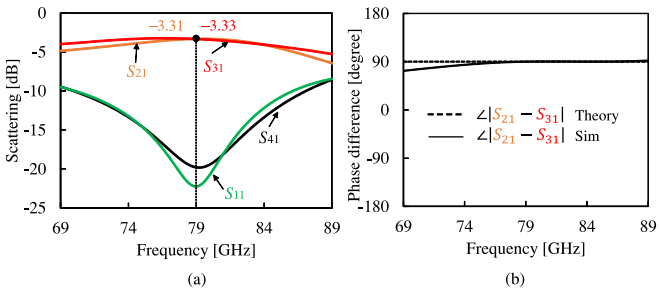

FIGURE 12. Simulated characteristics of hybrid coupler. (a) Scattering parameters, (b) phase difference.

as -3.3 dB. Therefore, insertion loss is estimated as approximately 0.3 dB. The phase difference of the hybrid coupler output ports is indicated in Fig. 12(b). The result shows an agreement with the theory with the phase difference of output port 2 and port 3 is 90.3°.

A crossover is a cascade connection of two hybrid couplers with the impedance characteristic Z_0 of all branch lines. Power is transmitted from input port 1 to output port 3 without transmission to port 2 and port 4. The crossover is laid out at the middle metal pattern of the double-layer substrate as shown in Fig. 11(b). The electrical length of branch-lines are set to be $l_{c1} = l_{c2} = 0.88$ mm with the slotline gap $g_1 = 0.1$ mm. Similar to the hybrid coupler design, space in the square of crossover is not suitable to arrange some via holes $\phi_1 = 0.3$ mm with pitch of holes $c = 0.6$ mm. In this design, to ensure a unique distance of 0.2 mm between via holes and slotlines, via holes with $\phi_3 = 0.50$ mm are placed in the crossover square. The simulated scattering parameters of crossover is presented in Fig. 13. The insertion loss is 0.8 dB at 79 GHz. Isolations are achieved at port 2 and port 4 with the amplitude below -25 dB. The overlapped bandwidth of the designed hybrid coupler and crossover is 15% for $|S_{11}| < -10$ dB (from 74 GHz to 86 GHz).

In this Butler matrix, two phase shifters with 0° and 45° phase adjustment are designed to compensate the phase difference of the adjacent crossovers. The phase difference is controlled by introducing a line offset ΔL as shown in Fig. 11(c). The simulated results of phase shifters are shown

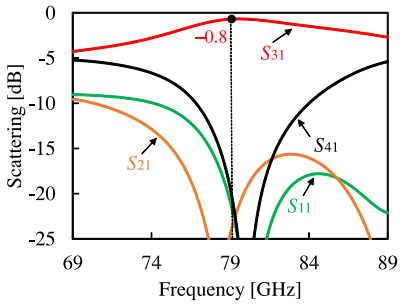

FIGURE 13. Simulated scattering parameters of crossover.

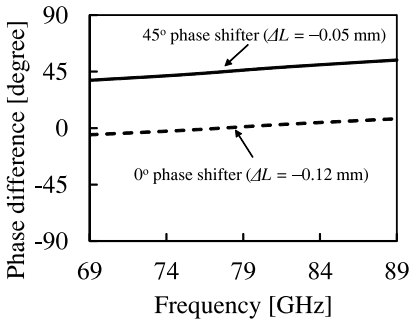

FIGURE 14. Simulated phase difference of phase shifters.

in Fig. 14. The line offset is estimated as $\Delta L = -0.12$ mm for 0° phase adjustment and $\Delta L = -0.05$ mm for 45° phase adjustment. The optimum parameters of the Butler matrix components are presented in Table 2.

The designed Butler matrix components and waveguide-to-finline transition using the proposed finline are integrated together to form a comprehensive Butler matrix with feeding circuits as demonstrated in Fig. 15. The dimensions of the Butler matrix itself are 5×12 mm. Port #1, #2, #3 and #4 are the input ports; while port #5, #6, #7 and #8 are the output ports. The input ports and output ports of the Butler matrix are extended outward for convenient arrangement of transitions. In addition, since three types of vias have been used to design the appropriate structures of the hybrid couplers, crossovers, and phase shifters, six types of finlines are produced in the Butler matrix as shown in Fig. 16. This will cause the asymmetrical structures of the hybrid couplers in the Butler matrix that can be seen in Fig. 15. Characteristics of various finlines are investigated by simulation as demonstrated in Fig. 17. Although the investigated finlines have the same length of 1 cm, the transmission amplitude and phase show a slight difference between finlines. The maximum phase shift of 9° can be seen between finline F1 and F3. The transmission phase deviation of finlines affect the progressive phase shift of the Butler matrix output ports which will be discussed in Section B. The simulated and measured performance of the Butler matrix are also compared and discussed in next subsection.

B. SIMULATED AND MEASURED RESULTS

A fabricated prototype of the Butler matrix using the proposed finline is shown in Fig. 18. Two substrates

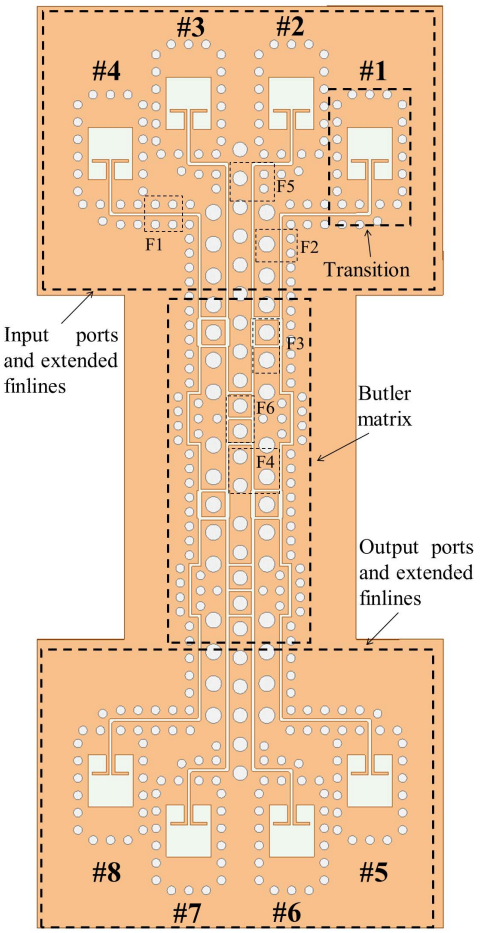

FIGURE 15. Geometry of the proposed finline Butler matrix with transitions.

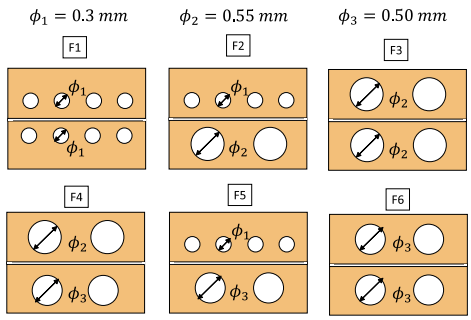

FIGURE 16. 6 types of finlines in the proposed Butler matrix.

consisting of three metal plates are sticked together by heating technology. The Butler matrix is constructed on the middle metal layer and fed from the waveguide through an aperture located on the bottom metal layer. The measurement of scattering characteristics are conducted by MS4647B-ANRITSU Vector Network Analyzer (VNA). Due to the small-scale prototype, 2 of 8 ports are connected to the VNA at the same time for measurement, the rest terminals are covered by waveguide absorber.

The measured and simulated reflection characteristics of the Butler matrix ports $|S_{11}|$, $|S_{22}|$, $|S_{55}|$ and $|S_{66}|$ are

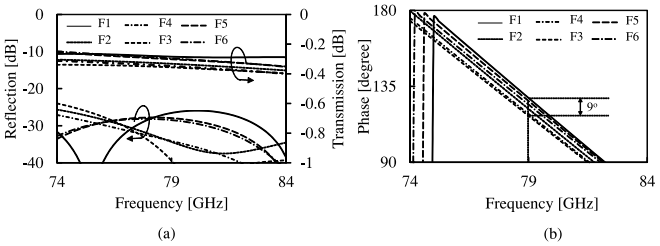

FIGURE 17. Characteristics of 6 types of finlines. (a) S-parameter, (b) Transmission phase.

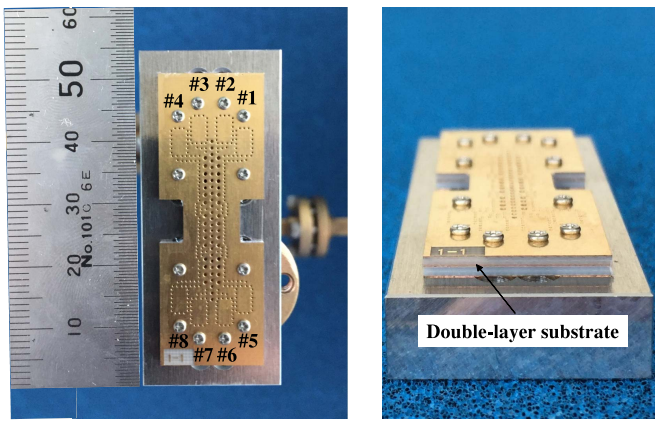

FIGURE 18. Fabricated prototype of Butler matrix using finline in double-layer substrate. (a) Upper view, (b) Side view.

illustrated in Figs. 19. In the measured results, many ripples appear because of the effect of multi-reflection of the fabricated prototype in the measurement. However, the reflection characteristics almost show the agreement between measured and simulated results. A slight shift of 0.6 GHz can be seen between measurement and simulation in $|S_{22}|$ and $|S_{55}|$ which is because of fabrication tolerance. $|S_{44}|$, $|S_{33}|$, $|S_{88}|$ and $|S_{77}|$ should be similar to $|S_{11}|$, $|S_{22}|$, $|S_{55}|$ and $|S_{66}|$, respectively due to the symmetrical geometry of the Butler matrix. The input ports show the overlapped bandwidth of 11% for the reflection level less than −10 dB (from 74 to 82.5 GHz).

The simulated and measured amplitude of output ports when alternating the input excitation are exhibited in Fig. 20. In this measurement, the effect of multi-reflection in fabricated prototype makes it difficult to estimate the amplitude of output ports since many ripples appear in the measured curves. Therefore, gating function in time domain is utilized to reduce unwanted reflections [28], making the amplitude curves smooth but do not change the amplitude values. At most output ports, the measured and simulated transmission amplitudes agree with each other with the amplitude higher than −10 dB at 79 GHz, however, they tend to decrease at higher frequencies. By alternating excitation of port 1, 2, 3 and 4, the common frequency bandwidth in which the transmission amplitude is higher than −10 dB is around 5 GHz (from 74 to 79 GHz).

The amplitude distributions at the output ports at 79 GHz are described in Fig. 21. Since −6 dB is the theoretical

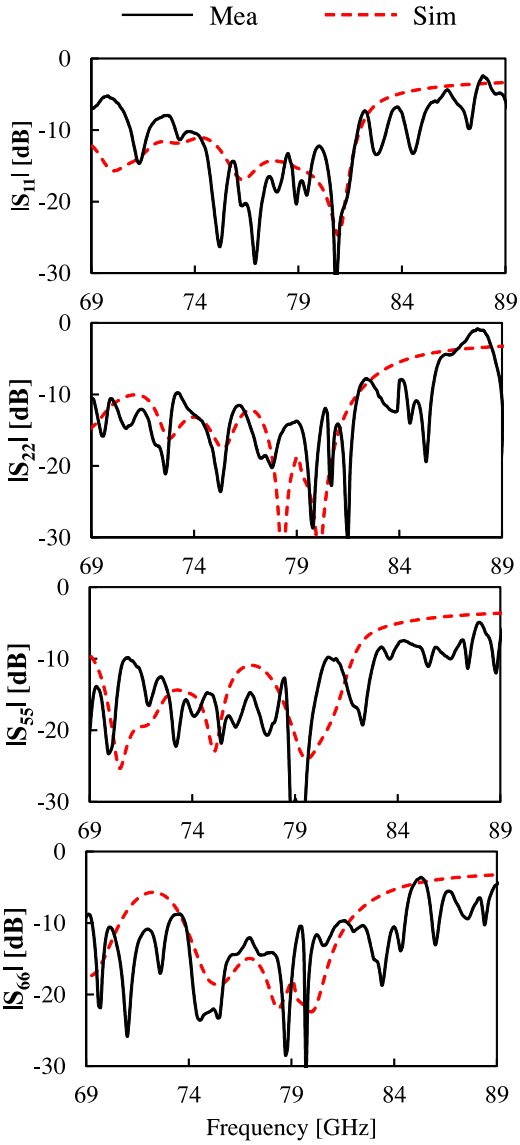

FIGURE 19. Measured and simulated reflection characteristics of the Butler matrix ports.

uniform amplitude dividing to 4 output ports, measured amplitudes of the output ports fluctuate between −10 dB and −8 dB when each input port is excited, while simulated results are between −9 dB and −6 dB. The amplitude imbalance of output ports is mainly due to the asymmetrical structures of the hybrid couplers in the Butler matrix as shown in Fig. 15. Compared to the lossless Butler matrix in theory, the deterioration of amplitude is caused by insertion loss of the measured Butler matrix. They are calculated as 2.96 dB, 3.18 dB, 3.27 dB and 3.02 dB, corresponding to excitations of input ports #1, #2, #3 and #4, respectively. Therefore, the average insertion loss of the proposed Butler matrix is calculated approximately 3.1 dB. In the measured results, the loss includes the insertion loss of the Butler matrix itself and the insertion loss of two waveguide-to-finline transitions for input and output ports. Therefore, with the insertion loss of each transition is 0.34 dB as discussed

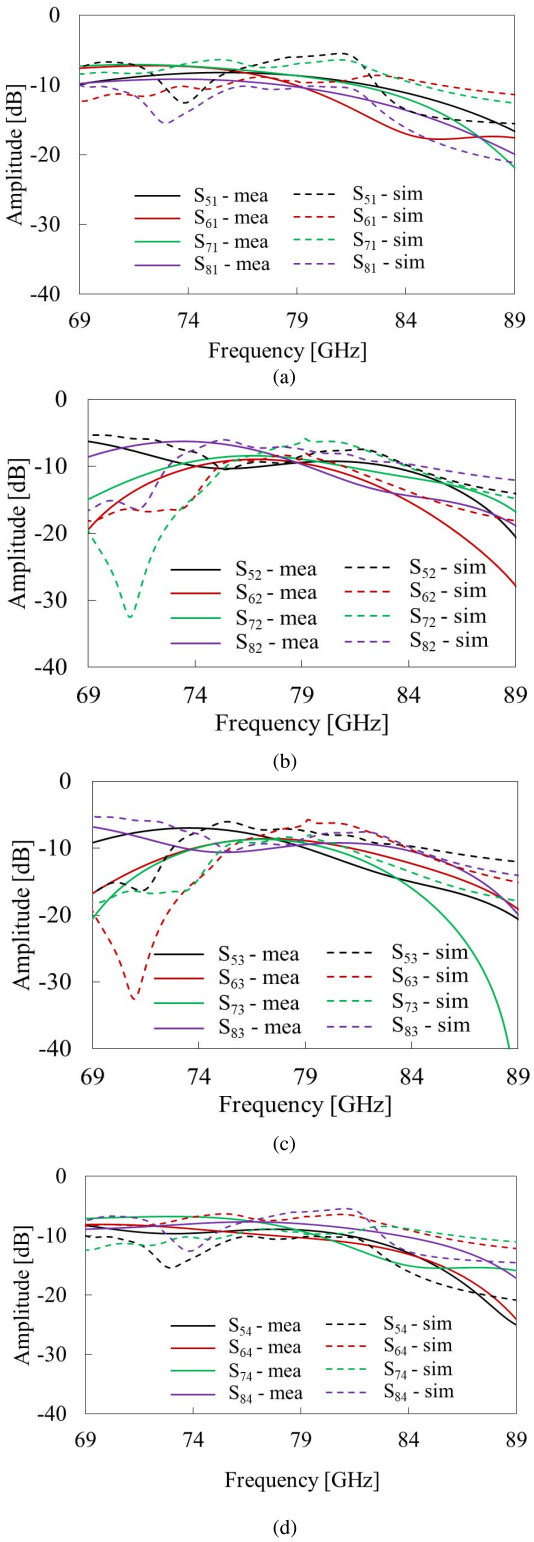

FIGURE 20. Measured and simulated amplitude of output ports. (a) when port 1 is excited, (b) when port 2 is excited, (c) when port 3 is excited, (d) when port 4 is excited.

in Section II, the insertion loss of the Butler matrix itself is estimated as 2.42 dB.

In term of transmission phase, the phase difference between adjacent output ports for the port i excitation is

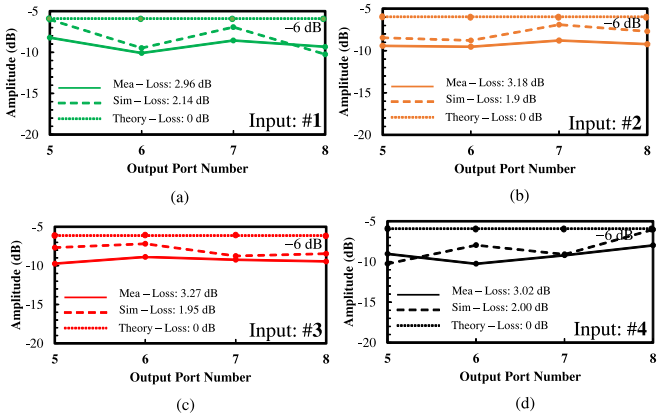

FIGURE 21. Measured and simulated amplitude of output ports at 79 GHz. (a) when port 1 is excited, (b) when port 2 is excited, (c) when port 3 is excited, (d) when port 4 is excited.

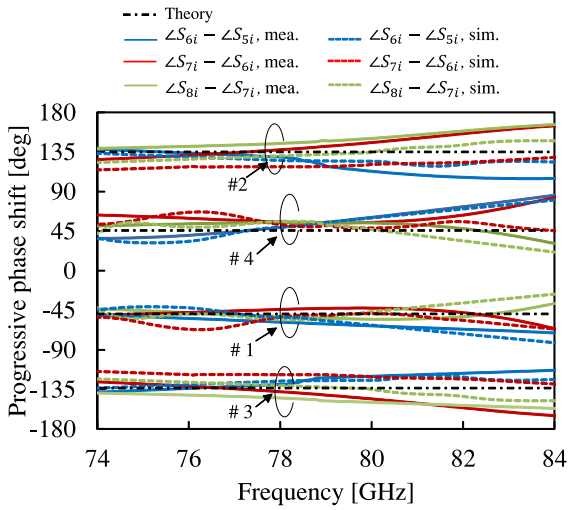

FIGURE 22. Progressive phase shifts of the Butler matrix output ports when port i is excited ($i = 1, 2, 3, 4$).

theoretically given by:

$$\phi_i = \pm\frac{(2p-1)}{N} \times \pi \tag{1}$$

where N is the order of the Butler matrix ($N = 2^n$) [11]. In this Butler matrix, $N = 4$, $n = 2$ and $p = 1, \ldots, n$. Hence, the phase differences of Butler matrix output ports are $\pm 45°$ for port 1 and port 4 excitation and $\pm 135°$ for port 2 and port 3 excitation. Figure 22 further describes progressive phase shifts of the Butler matrix output ports when port i is excited ($i = 1, 2, 3, 4$). The agreement can be seen between measured and simulated phases. In the measurement, the maximum phase error is 16° at the designed frequency of 79 GHz. The phase deviation is mainly due to the accumulated phase errors of the Butler matrix components those are composed of various finlines as discussed in Fig. 17.

Finally, for the radiation pattern, the array factor of the proposed Butler matrix is then calculated from the obtained results of the transmission amplitude and transmission phase

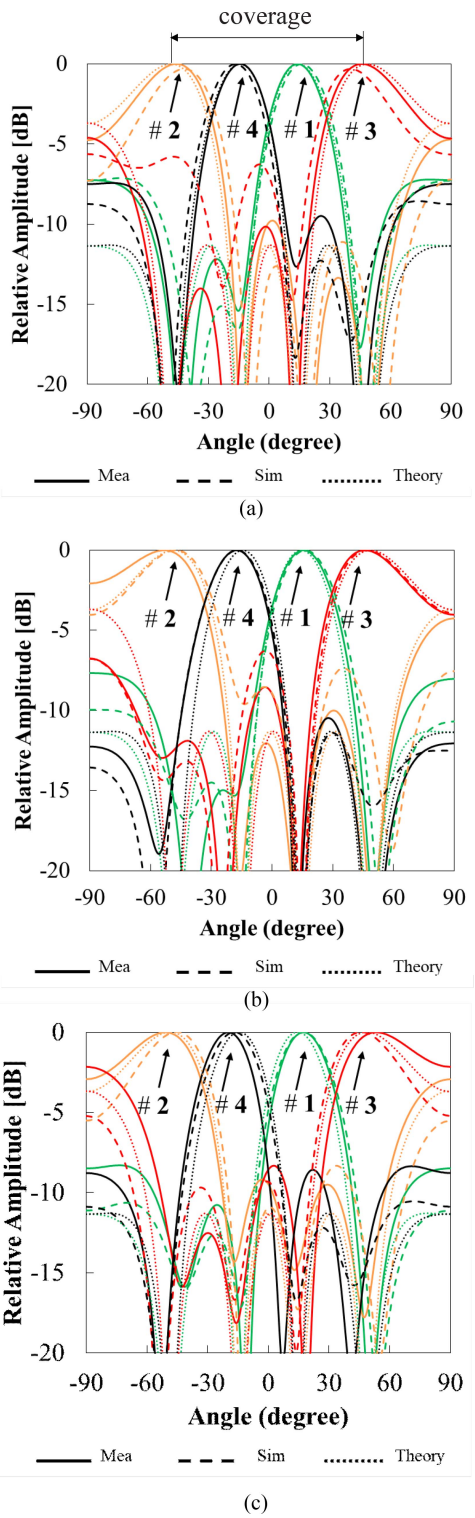

FIGURE 23. Array factors for element spacing of half wavelength. (a) 79 GHz, (b) 76 GHz, (c) 82 GHz.

by following equation [29]:

$$AF[\theta, \phi_i] = \frac{sin\left(N\left[\frac{d\pi}{\lambda} sin(\theta) - \frac{\phi i}{2}\right]\right)}{Nsin\left(\frac{d\pi}{\lambda} sin(\theta) - \frac{\phi i}{2}\right)} \quad (2)$$

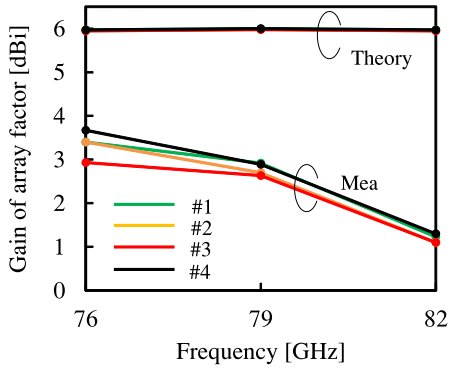

FIGURE 24. Gain versus frequency of array factor.

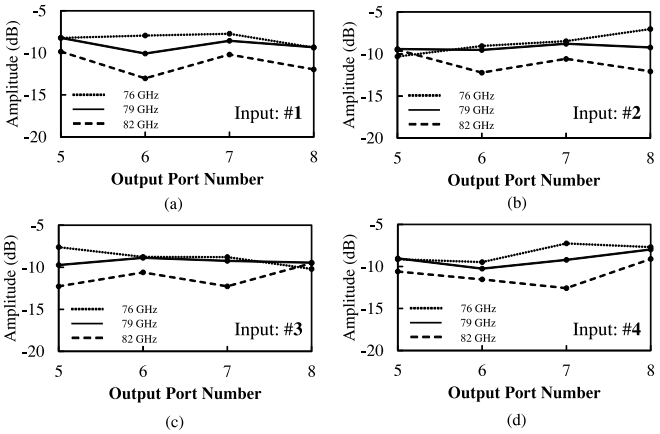

FIGURE 25. Measured amplitude of Butler matrix at 76 GHz, 79 GHz and 82 GHz. (a) Port 1 is excited, (b) port 2 is excited, (c) port 3 is excited, (d) port 4 is excited.

In this calculation, the radiation elements are assumed 4 isotropic antennas ($N = 4$) and spacing between elements is a half-wavelength each ($d = \lambda/2$). θ is the direction angle of the array factor and ϕ_i indicates the phase difference between adjacent output ports. The calculated array factor at the desired frequency of 79 GHz and its neighboring frequencies of 76 GHz and 82 GHz are shown in Fig. 23. Four directional beams are produced by the proposed Butler matrix and the beam directions show that a slight difference is witnessed between measured data and theoretical data due to phase error in the fabricated Butler matrix. The direction angles of 4 beams are calculated by MATLAB using Eq. (2). At the desired frequency of 79 GHz, measured results show that the beam directions are $+14°$, $-46.5°$, $+46.5°$ and $-14°$ for the excitation of port 1, 2, 3, and 4, respectively, as described in Fig. 23(a). The maximum angle deviation of 2.5° can be seen between measured and theoretical results. Similarly, 4 directional beams are also generated in array factors at 76 GHz and 82 GHz with the maximum angle deviation of 5.5° and 7° as presented in Fig. 23(b) and Fig. 23(c), respectively.

On the other hand, the gain of 4 beams assuming isotropic elements at the center frequency of 79 GHz and neighbor frequencies of 76 GHz and 82 GHz are presented in Fig. 24.

TABLE 3. Comparison between proposed and developed Butler matrix.

Ref.	Butler matrix	f_c (GHz)	Coverage (peak direction)	Insertion loss (dB)	Technology
[12]	64×64	20	40% hemisphere	1.8	WG
[13]	4×4	0.9	$-66°$ to $+66°$	2.6	PCB
[14]	4×4	30	$-56°$ to $+51°$	n.a	SIW
[15]	8×8	61	$-49°$ to $+49°$	3.1	CMOS
[16]	8×8	2.2	$-44°$ to $+44°$	3.6	Multilayer stripline
This work	4×4	79	$-46.5°$ to $+46.5°$	2.42	Finline

The measured transmission losses of the Butler matrix are indicated in Fig. 25. Due to the transmission loss of the Butler matrix, the gain at 79 GHz is about 3 dBi and it is degraded about 3 dB compared to the theoretical gain. At 76 GHz, the gain of 4 beams varies between 3 dBi and 3.6 dBi. As can be seen in Fig. 25, the transmission losses at 82 GHz increase by approximately 2 dB compared to the losses at 79 GHz, followed by a reduction of gain at 82 GHz. The high losses can be explained by the high reflection level of the Butler matrix ports at 82 GHz as shown in Fig. 19. The gain is higher than 1 dBi at 82 GHz. Overall, the proposed Butler matrix generates 4 switchable beams with the gain of the array factor is approximately 3 dBi at the center frequency of 79 GHz.

C. COMPARISON AND DISCUSSION

The performance summary of the proposed and developed Butler matrices are compared in Table 3. Although each study was conducted by design frequencies and different processing techniques such as waveguide, PCB, SIW, CMOS chip and multilayer stripline, the fairest comparisons are given to evaluate the effectiveness of this study. The developed Butler matrix in [12] seems to obtain the performance of cover range as well as insertion loss because it was designed by the hollow waveguide processing technology. However, the structure seems complicated with high fabrication costs. Other reported Butler matrices are more simple structures but the insertion losses are also moderate. In this work, the Butler matrix is designed by proposed finline in double-layer dielectric substrate and waveguide-to-finline transitions. Four directional beams produced by the Butler matrix can be steered within a coverage range of peak direction between $-46.5°$ and $+46.5°$ as presented in Fig. 23. The insertion loss of the Butler matrix itself is acceptable as 2.42 dB. This advantage of the insertion loss would be a promising solution to design multibeam antennas with high directivity in the millimeter-wave band.

V. CONCLUSION

In this article, a wideband, low insertion loss millimeter-wave beamforming circuit of Butler matrix was proposed and investigated at 79 GHz by using finline in double-layer dielectric substrate. The proposed finline was constructed by a slotline inserted in the metal pattern between two dielectric substrate layers with two rows of via-hole arrangement. The closed structure of the finline resulted in low-loss transmission characteristic. In addition to that, a waveguide-to-finline transition structure was developed as a feeding circuit for the Butler matrix. The performance of the proposed Butler matrix was evaluated by electromagnetic simulator and confirmed by experimental results. In the measurement, the proposed Butler matrix obtained an acceptable insertion loss of 2.42 dB and 4 switchable beams were achieved with the beam directions of $+14°$, $-46.5°$, $+46.5°$ and $-14°$, respectively. With advantages of transmission performance, simple structure and low cost, the finline in double-layer substrate would be an attractive solution for millimeter-wave applications.

REFERENCES

[1] P. Wang, Y. Li, L. Song, and B. Vucetic, "Multi-gigabit millimeter wave wireless communications for 5G: From fixed access to cellular networks," *IEEE Commun. Mag.*, vol. 53, no. 1, pp. 168–178, Jan. 2015.

[2] T. Rappaport *et al.*, "Millimeter wave mobile communications for 5G cellular: It will work!" *IEEE Access*, vol. 1, pp. 335–349, 2013.

[3] W. Menzel, D. Pilz, and R. Leberer, "A 77-GHz FM/CW radar front-end with a low-profile low-loss printed antenna," *IEEE Trans. Microw. Theory Techn.*, vol. 47, no. 12, pp. 2237–2241, Dec. 1999.

[4] H. Sharifi *et al.*, "Semi-transparent and conformal antenna technology for millimeter-wave intelligent sensing," in *Proc. IEEE MTT-S Int. Conf. Microw. Intell. Mobility (ICMIM).*, Munich, Germany, 2018, pp. 1–4.

[5] R. Feger, A. Haderer, and A. Stelzer, "Experimental verification of a 77-GHz synthetic aperture radar system for automotive applications," in *Proc. IEEE MTT-S Int. Conf. Microw. Intell. Mobility (ICMIM)*, Nagoya, Japan, 2017, pp. 111–114.

[6] M. Murad, J. Nickolaou, G. Raz, J. S. Colburn, and K. Geary, "Next generation short range radar (SRR) for automotive applications," in *Proc. IEEE Radar Conf.*, Atlanta, GA, USA, 2012, pp. 0214–0219.

[7] J. Blass, "Multidirectional antenna—A new approach to stacked beams," in *Proc. IRE Nat. Conv. Rec.*, New York, NY, USA, 1958, pp. 48–50.

[8] S. Mosca, F. Bilotti, A. Toscano, and L. Vegni, "A novel design method for Blass matrix beam-forming networks," *IEEE Trans. Antennas Propag.*, vol. 50, no. 2, pp. 225–232, Feb. 2002.

[9] K. Sakakibara, S. Kitanaka, Y. Otsuka, N. Kikuma, and K. Iwasa, "Design of 2D Rotman-lens multi-beam antenna using multi-layer substrate integrated waveguide," in *Proc. IEEE MTT-S Int. Conf. Microwav. Intell. Mobility (ICMIM)*, Munich, Germany, 2018, pp. 79–82.

[10] D. A. Williams, "Millimetre wave radars for automotive applications," in *IEEE MTT-S Int. Microw. Symp. Dig.*, vol. 2. Albuquerque, NM, USA, Jun. 1992, pp. 721–724.

[11] J. Butler and R. Lowe, "Beam forming matrix simplifies design of electronically scanned antennas," *Electron. Design*, vol. 9, pp. 170–173, Apr. 1961.

[12] T. Tomura, D. Kim, M. Wakasa, Y. Sunaguchi, J. Hirokawa, and K. Nishimori, "A 20-GHz-band 64 × 64 hollow waveguide two-dimensional butler matrix," *IEEE Access*, vol. 7, pp. 164080–164088, 2019.

[13] C.-W. Wang, T.-G. Ma, and C.-F. Yang, "A new planar artificial transmission line and its applications to a miniaturized butler matrix," *IEEE Trans. Microw. Theory Techn.*, vol. 55, no. 12, pp. 2792–2801, Dec. 2007.

[14] Q.-L. Yang, Y.-L. Ban, J.-W. Lian, Z.-F. Yu, and B. Wu, "SIW Butler matrix with modified hybrid coupler for slot antenna array," *IEEE Access*, vol. 4, pp. 9561–9569, 2016.

[15] T.-Y. Chin, J.-C. Wu, S.-F. Chang, and C.-C. Chang, "A V-band 8 × 8 CMOS Butler matrix MMIC," *IEEE Trans. Microw. Theory Techn.*, vol. 58, no. 12, pp. 3538–3546, Dec. 2010.

[16] C.-C. Chang, R.-H. Lee, and T.-Y. Shih, "Design of a beam switching/steering Butler matrix for phased array system," *IEEE Trans. Antennas Propag.*, vol. 58, no. 2, pp. 367–374, Feb. 2010.

[17] J. B. Knorr and P. M. Shayda, "Millimeter-wave fin-line characteristics," *IEEE Trans. Microwav. Theory Techn.*, vol. 28, no. 7, pp. 737–743, Jul. 1980.
[18] D. Mirshekar-Syahkal and J. B. Davies, "An accurate, unified solution to various fin-line structures, of phase constant, characteristic impedance, and attenuation," *IEEE Trans. Microwav. Theory Techn.*, vol. 30, no. 11, pp. 1854–1861, Nov. 1982.
[19] C. Schieblich, J. K. Piotrowski, and J. H. Hinken, "Synthesis of optimum finline tapers using dispersion formulas for arbitrary slot widths and locations," *IEEE Trans. Microwav. Theory Techn.*, vol. 32, no. 12, pp. 1638–1645, Dec. 1984.
[20] L. Golonka, P. Bembnowicz, D. Jurkow, K. Malecha, H. Roguszczak, and R. Tadaszak, "Low temperature co-fired ceramics (LTCC) microsystems," *Optica Applicata*, vol. XLI, no. 2, pp. 383–388, 2011.
[21] N. T. Tuan, K. Sakakibara, N. Kikuma, K. Iwasa, T. Okunaga, and A. Nakatsu, "Design of millimeter-wave 4 × 4 Butler matrix using finline in double layer dielectric substrate," in *Proc. Malaysia-Jpn Workshop Radio Technol. (MJWRT)*, Kuala Lumpur, Malaysia, 2019, pp. 1–2.
[22] N. T. Tuan, K. Sakakibara, N. Kikuma, K. Iwasa, T. Okunaga, and A. Nakatsu, "Design of millimeter-wave 4 × 4 Butler matrix using finline in double layer dielectric substrate," in *Proc. Soc. Conf.*, 2019, p. 1.
[23] N. T. Tuan, K. Sakakibara, N. Kikuma, K. Iwasa, T. Okunaga, and A. Nakatsu "Design of millimeter-wave 4 × 4 Butler matrix using finline in double layer dielectric substrate," in *Proc. Asia Pac. Conf. (AP)*, 2019, pp. 1–4.
[24] K. Sakakibara, N. T. Tuan, S. Yamauchi, S. Mariyama, and N. Kikuma "Multibeam antennas using multi-layer substrate in millimeter wave band," in *Proc. IEEE Asia–Pac. Conf. Appl. Electromagn. (APACE)*, Malacca, Malaysia, 2019, pp. 1–3.
[25] K. Sakakibara, Y. Mizuno, N. Kikuma, and K. Iwasa "Millimeter-wave 4 × 4 Butler matrix for feeding circuit of multi-beam antenna using finline in multilayer substrate," in *Proc. 12th Eur. Conf. Antennas Propag. (EuCAP)*, London, U.K., 2018, pp. 1–4.
[26] *HFSS. Ver. 17.2*, Ansoft Corp., Pittsburgh, PA, USA, 2017.
[27] *PILLAR PC-CLAD High Frequency Multi-Layer Boards*, Nippon Pillar Packing Co., Ltd, Osaka, Japan, 2013.
[28] J. Dunsmore, "Gating effects in time domain transforms," in *Proc. 72nd ARFTG Microw. Meas. Symp.*, Portland, OR, USA, 2008, pp. 1–8.
[29] P. Delos, B. Broughton, and J. Kraft, "Linear array: Beam characteristics and array factor," *Analog Dialogue*, vol. 54, no. 2, pp. 26–32, May 2020.

NGUYEN THANH TUAN (Graduate Student Member, IEEE) was born in Hanam, Vietnam, in 1991. He received the B.S. degree in electronics and telecommunication from the Hanoi University of Science and Technology, Hanoi, Vietnam, in 2014, and the M.S. degree in electronic systems from University Technology Malaysia, in 2017. He is currently pursuing the Ph.D. degree with the Department of Electrical and Mechanical Engineering, Nagoya Institute of Technology, Nagoya, Japan. His current research interests include the beamforming network for millimeter-wave antennas, and IC chip transitions.

KUNIO SAKAKIBARA (Senior Member, IEEE) was born in Aichi, Japan, in 1968. He received the B.S. degree in electrical and computer engineering from Nagoya Institute of Technology, Nagoya, Japan, in 1991, and the M.S. and D.E. degrees in electrical and electronic engineering from the Tokyo Institute of Technology, Tokyo, Japan, in 1993 and 1996, respectively.

From 1996 to 2002, he was with Toyota Central Research and Development Labs, Inc., Nagakute, where he was involved in the development of antennas for automotive millimeter-wave radar systems. From 2000 to 2001, he was a Guest Researcher with the Department of Microwave Techniques, University of Ulm, Ulm, Germany. In 2002, he joined the Nagoya Institute of Technology as a Lecturer. Since 2004, he has been an Associate Professor and he became a Professor with Nagoya Institute of Technology in 2012. His current research interests include millimeter-wave antennas and feeding circuits.

KOJIRO IWASA was born in Hiroshima, Japan, in 1992. He received the B.S. degree from the Department of Mechanical and Electrical Engineering, National Institute of Technology, Kure College. He started his career with Nippon Pillar Packing Company Ltd., in 2014, as an Engineer. He currently works on development of PTFE substrate suitable for mm-wave application thanks to its low transmission loss.

TAKESHI OKUNAGA was born in Shiga, Japan, in 1981. He started his career with Nippon Pillar Packing Company Ltd., in 2006, as an Engineer. He has been in charge of millimeter-wave antennas design and evaluation. He has over ten years experience in this field. He is currently a Chief Engineer and responsible for developing PTFE substrate especially for high frequency application.

NOBUYOSHI KIKUMA (Senior Member, IEEE) was born in Ishikawa, Japan, in 1960. He received the B.S. degree in electronic engineering from the Nagoya Institute of Technology, Japan, in 1982, and the M.S. and Ph.D. degrees in electrical engineering from Kyoto University, Japan, in 1984 and 1987, respectively.

From 1987 to 1988, he was a Research Associate with Kyoto University. In 1988, he joined the Nagoya Institute of Technology, where he has been a Professor since 2001. His current research interests include adaptive and signal processing array, multipath propagation analysis, mobile and indoor wireless communication, and electromagnetic field theory.

Prof. Kikuma was a recipient of the 4th Telecommunications Advancement Foundation Award in 1989.

YOSHIKI SUGIMOTO (Member, IEEE) was born in Fukui, Japan. He received the B.Sc. and M.Sc. degrees from the University of Fukui, Fukui, in 2013 and 2015, respectively, and the Ph.D. degree from Yokohama National University, Yokohama, Japan, in 2018. From 2018 to 2020, he was with Omron Corporation. In 2020, he joined the Nagoya Institute of Technology as an Assistant Professor. His research interest includes antenna measurement and scattering problems.